

# Lattice Vibrations of Boron Carbides

P. A. Medwick<sup>1</sup> and R. O. Pohl<sup>2</sup>

*Laboratory of Atomic and Solid State Physics, Cornell University, Ithaca, New York 14853*

Received January 21, 1997; accepted February 6, 1997

The internal friction at low temperatures has been measured on polycrystalline samples of  $\beta$ -B,  $B_4C$ ,  $B_{13}C_2$ , and  $B_9C$ . As the carbon deficiency increases in the boron carbides, the internal friction approaches that of amorphous solids. For comparison, the internal friction of amorphous  $B_9C$ , produced as a thin film by e-beam evaporation on a Si double-paddle oscillator, has also been measured. It is very similar to that of the polycrystalline  $B_9C$  sample. The results are discussed in terms of glass-like lattice vibrations which have been noted before in highly disordered crystals, e.g.,  $Ba_{1-x}La_xF_{2x}$ . It is concluded that the low thermal conductivity of  $B_9C$  near room temperature which has been observed previously is indeed equal to its theoretical lower limit. © 1997 Academic Press

## I. INTRODUCTION

In a previous publication (1), it was shown that the thermal conductivity of crystalline  $B_9C$  near room temperature resembles that of amorphous solids. This led to the suggestion that the lattice vibrations of this compound differed in a very characteristic way from those of many common crystalline solids, rather resembling those of amorphous solids. This paper contains further evidence in support of this earlier conclusion.

After describing the experimental techniques and the materials to be studied, the basic differences between the lattice vibrations of crystalline and amorphous solids will be briefly reviewed. This will be followed by measurements of the internal friction of polycrystalline  $B_4C$ ,  $B_{13}C_2$ , and  $B_9C$ . The findings for the latter will be compared with measurements of an amorphous  $B_9C$  film.

## II. EXPERIMENTAL MATTERS

The  $c$ - $B_{13}C_2$  and  $c$ - $B_9C$  samples were hot-pressed (2450 K, 410 atm) by Dr. T. L. Aselage of Sandia National

Laboratories from boron and graphite powders under an argon atmosphere in a graphite die lined with BN (2). The  $c$ - $B_{13}C_2$  ( $\rho = 2.47 \text{ g cm}^{-3}$ ) and  $c$ - $B_9C$  ( $\rho = 2.46 \text{ g cm}^{-3}$ ) samples were similar to those prepared for the thermal conductivity measurements reported previously (1) and were nearly fully dense ( $> 98\%$  of theoretical density). Samples were examined by X-ray diffraction and Raman spectroscopy to confirm good crystallinity, absence of secondary phases, and absence of carbon diffusion into the material from the graphite die (2, 3). Samples previously prepared using this procedure for the earlier study (1) had grain sizes ranging from approximately 10–20  $\mu\text{m}$  (for carbon-rich samples;  $x \sim 0.20$ ) to 50–60  $\mu\text{m}$  (for carbon-deficient samples;  $x \sim 0.10$  (4)). The sample of hot-pressed  $c$ - $B_4C$  ( $\rho = 2.37 \text{ g cm}^{-3}$ , grain size  $\sim 3 \mu\text{m}$ ) was obtained from F. Thevenot; it had been pressed from an ESK (Electroschmelzwerk Kempten) pure arc-melted boron powder and was  $\sim 93\%$  fully dense. The polycrystalline  $\beta$ -B ( $\rho = 2.33 \text{ g cm}^{-3}$ ) was obtained from Hughes Research Laboratories; details of its fabrication are unknown. Due to the extreme hardness of  $c$ - $B_{1-x}C_x$ , electro-disintegration (spark cutting) was used to cut the samples into the rectangular prismatic geometry required for the composite oscillator technique (described next).

The internal friction of these bulk samples was measured using the composite torsional oscillator technique of Cahill and Van Cleve (5). The sample, which was fashioned into a rectangular prismatic geometry, was bonded with an epoxy (Stycast 2850FT) to a cylindrical quartz piezoelectric transducer. Typical dimensions were  $\sim 0.3 \times 0.3 \times 2.54 \text{ cm}$ ; for the quartz piezo 0.4 cm diameter,  $\sim 1 \text{ cm}$  length. The composite oscillator was attached with epoxy to a BeCu pedestal mount. Oscillations of the composite torsion bar were excited via a quadrupolar electrode assembly which surrounded the transducer; the torsion axis was along the long dimension of the oscillator. The lengths of transducer and sample were appropriately chosen such that the epoxy bond between the two was located at a displacement antinode (and therefore a stress node) for the fundamental torsion mode at the desired frequency ( $\sim 160 \text{ kHz}$  for this work). Details of the measurements and their evaluation will be described elsewhere (6).

<sup>1</sup> PPG Industries Inc., Glass Technology Center, P.O. Box 11472, Pittsburgh, PA 15238-0472.

<sup>2</sup> To whom correspondence should be addressed. E-mail: Pohl@msc.cornell.edu.

The amorphous  $a\text{-B}_9\text{C}$  film was deposited onto a silicon double-paddle oscillator (described below) by electron beam evaporation. The substrate was thermally sunk to the vacuum vessel and kept approximately at room temperature during the deposition. A remnant of the hot-pressed  $c\text{-B}_9\text{C}$  sample from Sandia was used as source. Deposition parameters were base pressure  $\sim 1 \times 10^{-7}$  Torr, beam current 10 mA, beam voltage 18 kV, and deposition rate  $10 \text{ \AA s}^{-1}$ . Ion scattering analysis showed the carbon content to be between 9 and 10 at.%, close to the composition of the target material (10 at.%). Oxygen contamination was  $\sim 3.7$  at.%. Hydrogen contamination was less than 1 at.%. Film thickness was measured with stylus profilometry to be  $0.176 \mu\text{m}$ . The areal mass coverage was determined from Rutherford Backscattering Spectrometry. From these measurements, the mass density of the film was determined to be  $1.68 \text{ g cm}^{-3}$ , 68% of the theoretical bulk density of crystalline  $\text{B}_9\text{C}$  ( $2.48 \text{ g cm}^{-3}$  (1)). The bulk density of  $a\text{-B}$  is not known. The mass density of the amorphous phase is frequently smaller than that of the crystalline phase. For  $\text{SiO}_2$ , for which this difference is especially large, the density of the amorphous phase is 85% of that of quartz (2.2 vs  $2.6 \text{ g cm}^{-3}$ ). We therefore believe that part of the density difference observed for the  $a\text{-B}_9\text{C}$  film is caused by porosity.

The internal friction of the film was determined from the increase of the damping it caused when deposited on a silicon double-paddle oscillator which, because of its extreme purity (it is machined out of very pure Si wafers) and its geometry, had very small damping at low temperatures, as will be shown below. For details of the technique, see Refs. (7) and (6); the latter also contains details of the measurements.

### III. GLASS-LIKE LATTICE VIBRATIONS

The lattice vibrations of solids in the crystalline phase differ from those of the amorphous phase in a characteristic way. Here, we concentrate on two specific aspects which are important for the low temperature ( $< 10 \text{ K}$ ) elastic and thermal properties, and for the heat transport near  $300 \text{ K}$ , respectively. The lattice vibrations of both crystalline and amorphous solids are illustrated schematically in Fig. 1, which compares the density of states of the vibrational excitations. By ignoring the dispersion of the elastic waves, the density of states for the crystalline solid on a doubly logarithmic plot varies as a straight line with slope 2 (called the Debye model), up to a limiting cutoff frequency (Debye frequency), which, depending on the material, is on the order of  $10^{13} \text{ s}^{-1}$ . The important point is that all excitations are elastic waves, i.e., collective excitations in which neighboring atoms vibrate with fixed phase relations. In amorphous solids, similar excitations are also observed, but two modifications are noted. At low frequencies, additional loc-

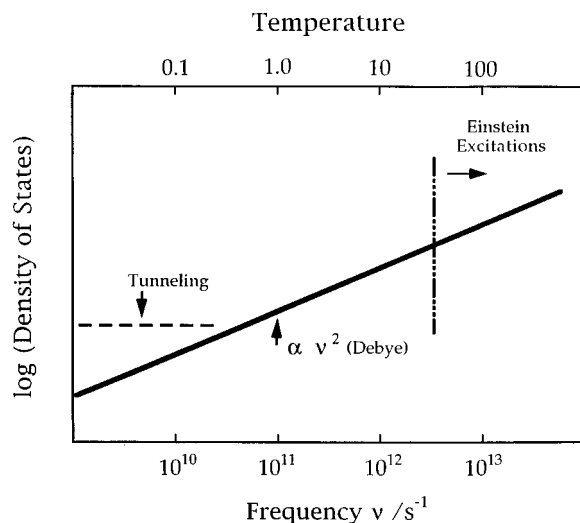


FIG. 1. Schematic comparison of the lattice vibrations of crystalline and amorphous solids. Doubly logarithmic plot. Both the tunneling states and Einstein excitations are characteristic of amorphous solids.

alized excitations exist; a model based on the assumption of tunneling states, with certain atoms tunneling between nearly equivalent positions, has been very successful in the description of the experimental results obtained on these excitations (8,9). The physical nature of these excitations, however is still unclear. Their density of states is nearly constant, as indicated in Fig. 1. These excitations cause the anomalous elastic and thermal properties observed in all amorphous solids including a thermal conductivity which varies as temperature squared below  $1 \text{ K}$ , and an internal friction which is frequency independent and independent of temperature over a wide temperature range below  $\sim 10 \text{ K}$ . Examples of both will be shown below. The most remarkable fact, however, is that the density of states of these tunneling excitations has nearly the same magnitude in all amorphous solids (10) (see also (6) for a recent compilation), an observation which remains unexplained (11).

The second difference is observed in measurements of the thermal conductivity above  $\sim 50 \text{ K}$ . Using the picture of elastic waves as heat carriers in amorphous solids leads to average phonon mean free paths on the order of the interatomic spacing, clearly an unphysical situation for waves whose shortest wavelength is of the same magnitude (12, 13). A more successful description of the heat transport in this temperature range is based on a model first proposed by Einstein (14) in which he assumed that every atom vibrates with random phases relative to its neighbors. In that case, he showed that the vibrational energy (heat) would propagate in a random walk from one atom to its neighbors. In this model, the thermal conductivity is determined by the jump distance (the average nearest neighbor distance of the

atoms) and the jump time, which he determined to be one half of the period of vibration (like the time of flight of an atom in a dense gas between collisions (15)). Although Einstein noticed that this model failed for crystalline solids, for the by now well-known reason that the heat is carried by waves in these solids (see Fig. 1), it has recently been observed that Einstein's model provides an excellent description for the thermal conductivity of amorphous solids (16). Since no unambiguous Einstein frequency can be determined from experiment, an interatomic average force constant was calculated from measured elastic constants. From this force constant, and the average atomic mass, an Einstein frequency, and, from it, the jump time, was determined. Although this is a rather crude method, it has the advantage of being unambiguous. With no adjustable parameters, the Einstein model leads to the right temperature dependence above  $\sim 50$  K and also to the right order of magnitude. The latter observation is illustrated in Fig. 2 which is taken from Ref. (17), updated with data for  $\alpha\text{-Bi}_2\text{Sr}_2\text{CaCu}_2\text{O}_8$ ,  $\alpha\text{-H}_2\text{O}$ ,  $\alpha\text{-Si}_3\text{N}_4$ ,  $\alpha\text{-TiO}_2$ , and  $\alpha\text{-B}$  (see also Table 1). Figure 2 shows a comparison of the calculated thermal conductivity at 300 K for all amorphous solids with reasonably small mol-

ecules (i.e., excluding polymers), for which the thermal conductivity has been measured (the solid circles; the open circles are for disordered crystals which will be mentioned shortly). Over a factor of 10 in magnitude, the experimental data are close to the dashed line which indicates perfect agreement with Einstein's model. Given the simple picture used to determine jump time and jump distance, the agreement between theory and experiment appears adequate. It is taken as evidence for the existence of localized oscillators, which are highly damped at frequencies above several THz (as marked with the vertical dash-dot line in Fig. 1). We do not claim that plane (Debye) waves do not exist at these elevated temperatures, but simply note that their contribution to the heat flow is small; for a critical experimental investigation of this point, see (18). Similarly, we do not deny the existence of longer-lived localized excitations in amorphous solids, which are in fact evidenced through narrow IR optical absorption bands. We only note that their numbers do not seem to be large enough to lead to a noticeable reduction of the thermal conductivity, through an average decrease of the jump rate. We will return to this point later, when we discuss polycrystalline fullerene.

An important point to make in preparation for the subsequent discussion of  $\text{B}_{1-x}\text{C}_x$  is that by now many crystals have been identified whose lattice vibrations cannot be described by waves alone, but are in fact indistinguishable from structurally amorphous solids, at low, as well as at high frequencies, as illustrated in Fig. 1. Their lattice vibrations are referred to as "glass-like." This definition of what is called "glass-like" is possibly more restrictive than that suggested when the term was used previously (19), where it referred only to the low energy (tunneling) excitations. There is, however, no example known for which the tunneling and the localized Einstein oscillations have been found not to exist simultaneously (although in some cases, like for amorphous metals, there is no way of detecting such high frequency oscillations through measurements of the heat flow because the latter is dominated by electrons). Until such an example is found, we may assume that the two definitions are *de facto* identical. Among the crystals with glass-like lattice vibrations, only one class,  $\text{MB}_{66}$ , is nearly stoichiometric. Deviations from stoichiometry have no effect on the glass-like behavior (20). For these crystals,  $\sim 20\%$  of the boron atoms, those occupying nonicosahedral cages, are highly disordered (21). This disorder, in addition to the disorder in the arrangement of the  $M$  atoms (Y, Gd), may conceivably lead to the glass-like properties.

In some crystals, the transition from "crystal-like" (Debye) to "glass-like" lattice vibrations with increasing disorder has been studied. As an example, we show the mixed crystal  $\text{Ba}_{1-x}\text{La}_x\text{F}_{2+x}$ , which is produced by crystallizing a mixture of  $\text{BaF}_2$  and  $\text{LaF}_3$  (22). As the  $\text{La}^{3+}$  is incorporated substitutionally into a  $\text{Ba}^{2+}$  site, the excess  $\text{F}^-$  ion is placed onto an interstitial site in the simple cubic lattice

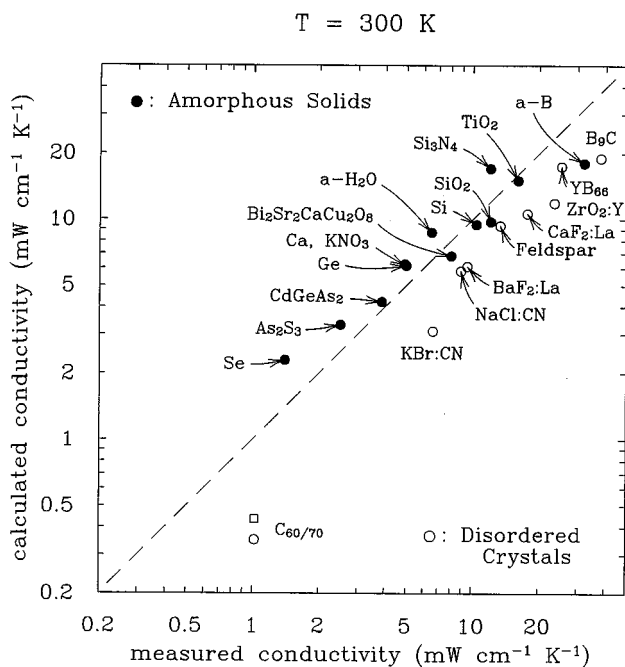


**FIG. 2.** Comparison of the values of the thermal conductivity calculated based on Einstein's model (also called minimum thermal conductivity,  $\Lambda_{\min}$ , as explained in text), with those measured on amorphous solids (solid circles) and on crystals with glass-like lattice vibrations (open circles), all at 300 K. Open square: See text. The sources of the data are given in Table 1. The dashed line indicates perfect agreement. Data points in the upper left triangle would indicate thermal conductivities smaller than those of the amorphous phase. Such conductivities do not seem to exist (all ordered or disordered crystals lead to data points in the right triangle).

formed by the  $F^-$  ions in the  $BaF_2$  lattice. The elastic and thermal effects of increasing  $x$  are illustrated in Figs. 3 and 4.

For small dopings,  $x \sim 10^{-2}$ , the low temperature internal friction increases only slightly (Fig. 3). However, increasing  $x$  leads to an increase in the internal friction, and to the formation of a plateau below 10 K, which for  $x = 0.33$  and  $x = 0.46$  is close to that of amorphous solids, with  $a\text{-SiO}_2$  shown as example. Note that the various peaks observed at higher temperature do not display such similarity. This observation does not support the picture that the relaxations probed above 10 K are closely connected with the tunneling states, and it justifies our choice of the low temperature tunneling states as the more common property of these solids. For a closer inspection of this point, see (23).

The thermal conductivity of pure  $BaF_2$ , Fig. 4, shows little evidence for defect scattering and is mainly determined by inelastic phonon-phonon scattering above the conductivity maximum and phonon-surface scattering below it (24). For  $x = 8 \times 10^{-3}$ , and somewhat more strongly in the mixed crystal of  $BaF_2$  and  $SrF_2$  (no excess  $F^-$ ), point defect scattering is observed (22). However, as  $x$  increases, the conductivity of  $Ba_{1-x}La_xF_{2+x}$  decreases drastically and approaches that of the structural glass,  $a\text{-SiO}_2$ . Note that the

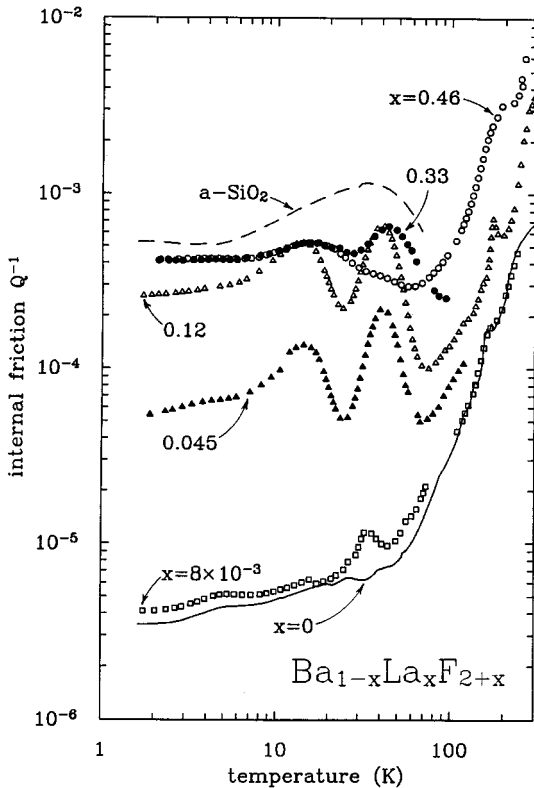


**FIG. 3.** Internal friction of  $Ba_{1-x}La_xF_{2+x}$  for increasing  $x$  approaches that characteristic of amorphous solids, with  $a\text{-SiO}_2$  shown for comparison. After (22).

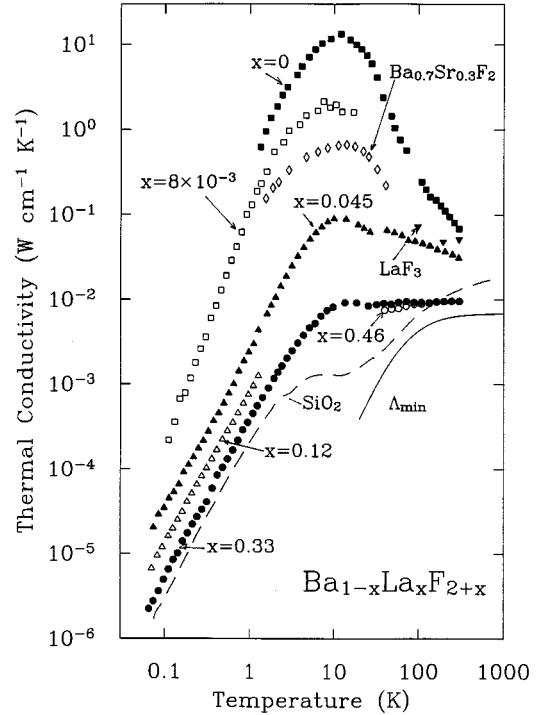


**FIG. 4.** Thermal conductivity of  $Ba_{1-x}La_xF_{2+x}$ , after (17). Note the relatively small effect of the addition of 30%  $SrF_2$  which does not lead to interstitial ions.

thermal conductivity for  $x = 0.46$  was only measured above 30 K, since this sample was slightly milky indicative of some precipitation, and hence additional scattering at grain boundaries had to be expected at lower temperatures. An example of such an effect has been shown in a glass ceramic (25). At high temperatures, however, the phonon mean free path becomes so short in the samples with large  $x$ , as the thermal conductivity approaches that predicted by the model based on Einstein's picture (labeled  $\Lambda_{min}$  in Fig. 4), that any additional scattering is irrelevant.

The comparison of  $\Lambda_{min}$  for  $Ba_{1-x}La_xF_{2+x}$ ,  $x = 0.33$  (at 300 K) with the measured thermal conductivity is shown in Fig. 2 (open circle). The other open circles are for all the other crystals in which glass-like lattice vibrations have been identified through measurements of the high temperature thermal conductivity. The references for all of these data are contained in (17), except for  $C_{60/70}$  and  $c\text{-B}_9C$  (the latter to be discussed in Section V).  $C_{60/70}$  consists of microcrystalline particles of fullerenes (buckyballs) compacted under pressure (26). No intentional chemical disorder had been introduced, and the presence of a small concentration of  $C_{70}$  (15%) was shown to be irrelevant (26). The most likely cause for the glass-like lattice vibrations for this solid is believed to be structural disorder caused during the compaction. A significant difference between these fullerene

compacts and all other disordered crystals with glass-like lattice vibrations is that the former showed no evidence for heat transport by intramolecular vibrations, which are 30 times more numerous than those of the rigid buckyballs (i.e., the thermal conductivity is temperature independent from 10 up to 300 K). Thus,  $\Lambda_{\min}$  (see Table 1) was calculated in this case assuming the buckyballs to be perfectly rigid, while for all other calculations for amorphous or crystalline solids in Fig. 2 every atom was considered in calculating the thermal conductivity.

Figure 2 shows two values for the calculated thermal conductivity of the fullerene compacts, shown as an open circle and an open square, respectively. The latter was calculated using the Einstein oscillator frequency as determined from the specific heat anomaly which in these compacts is well described by an Einstein function (26). Its origin is believed to be a translational as well as librational oscillation of the rigid buckyballs. The close agreement between the two values indicates that the determination of an Einstein frequency based on measurements of elastic constant, which has been used for all the other  $\Lambda_{\min}$  shown in Fig. 2, is at least a reasonable approximation.

One final point needs to be emphasized. In all attempts to lower the thermal conductivity of solids by increasing their chemical or physical disorder, short of making them porous (27), no conductivity has been reported to date to be smaller than that of the amorphous phase, i.e., no data points have been located in the upper left triangle delineated by the dashed line in Fig. 2 (data points for pure and disordered crystals occupy the right triangle). We take this fact as justification for our claim that the thermal conductivity of amorphous solids is the smallest possible thermal conductivity and will call the thermal conductivity calculated on the basis of Einstein's model, which appears to describe that of amorphous solids well, the minimum thermal conductivity,  $\Lambda_{\min}$ .

#### IV. ELASTIC MEASUREMENTS OF BORON CARBIDES

The internal friction of the piezoelectric quartz crystal oscillator is shown at the bottom of Fig. 5. Since the internal friction of the pure quartz crystal is probably much smaller, we believe that the measured internal friction is dominated by what is called "clamping losses" which include losses in

TABLE 1  
Parameters Used to Calculate the Minimum Thermal Conductivity  $\Lambda_{\min}$  at 300 K, as Described in (17)

	$n$ ( $10^{22} \text{ cm}^{-3}$ )	$v_t$ ( $10^5 \text{ cm/s}$ )	$v_l$ ( $10^5 \text{ cm/s}$ )	$\Lambda_{\min}$ (mW/cmK)	$\Lambda_{\text{meas}}$ (mW/cmK)
Amorphous					
$\text{Bi}_2\text{Sr}_2\text{CaCu}_2\text{O}_8$	7.18 <sup>a</sup>	2.092 <sup>a</sup>	3.225 <sup>a</sup>	6.8	8 <sup>b</sup>
$\text{H}_2\text{O}$	10.0	1.95 <sup>c</sup>	3.9 <sup>c</sup>	8.7	6.5 <sup>d</sup>
$\text{Si}_3\text{N}_4$	10.3	6.27 <sup>e</sup>	10.3 <sup>e</sup>	17	12 <sup>f</sup>
$\text{TiO}_2^g$	9.6	5.1	9.2	15	16
B	12.9	9.24 <sup>h</sup>	14.3 <sup>h</sup>	18	32 <sup>i</sup>
Disordered crystals					
c-B <sub>9</sub> C	13.4	7.342 <sup>j</sup>	12.098 <sup>j</sup>	19	38 <sup>k</sup>
$\text{C}_{60/70}^l$	0.083	1.9	3.3	0.35	1

Note.  $n$  is the number density of atoms, except for the fullerene compact, where it is the number density of the buckyballs, as explained in the text;  $v_t$  and  $v_l$  are measured transverse and longitudinal speeds of sound.  $\Lambda_{\text{meas}}$  is the measured thermal conductivity at 300 K. For none of the amorphous substances listed here, number densities and sound velocities are known for fully dense phases. Crystal data were used instead.

<sup>a</sup>H. Ledbetter, S. Kim, and K. Togano, *Physica C* **185–189**, 935 (1991).

<sup>b</sup>N. V. Zavaritsky, A. V. Samoilov, and A. A. Yurgens, *Physica C* **169**, 174 (1990).

<sup>c</sup>G. Simmons and H. Wang, "Single Crystal Elastic Constants and Calculated Aggregate Properties." MIT Press, Cambridge, MA, 1971. These are averaged velocities; the scatter is  $\sim \pm 3\%$ .

<sup>d</sup>O. Andersson and H. Suga, *Solid State Comm.* **91**, 985 (1994).

<sup>e</sup> $v_l$  was determined from the Young's modulus (B. E. While, private communication) and the elastic stiffness parameter (T. T. Retajczyk and A. K. Sinha, *Thin Solid Films* **70**, 241 (1980)).  $v_t$  was calculated from  $v_l$  using the empirical relation between the two quantities pointed out in (10).

<sup>f</sup>Our own measurements on a film produced at IBM (East Fishkill), with a chemical composition corresponding to a composition of roughly  $\text{H}_3\text{Si}_4\text{N}_5$ . Measurements on an atmospheric plasma CVD  $\text{SiN}_x$  film yielded  $14 \text{ mW cm}^{-1} \text{ K}^{-1}$ , while a plasma enhanced CVD  $\text{SiN}_x$  film yielded  $7.5 \text{ mW cm}^{-1} \text{ K}^{-1}$ . (S. M. Lee and D. G. Cahill, *J. Appl. Phys.* **81**, 2590 (1997)).

<sup>g</sup>D. G. Cahill and T. H. Allen, *Appl. Phys. Lett.* **65**, 309 (1994); speeds of sound of Rutile, as quoted in its Ref. (19).

<sup>h</sup>D. Gerlich and G. A. Slack, *J. Mater. Sci. Lett.* **4**, 639 (1985); measured on hot-pressed polycrystalline  $\beta$ -B.

<sup>i</sup>C. P. Talley *et al.*, in "Boron, Synthesis, Structure and Properties" (J. A. Kohn *et al.*, Eds., p. 94. Plenum, New York, 1960; see also (1).

<sup>j</sup>Gieske *et al.*, quoted in (1).

<sup>k</sup>(1).

<sup>l</sup>(26). Note that in Ref. (26), a  $\Lambda_{\text{Eins}}$  was calculated based on the Einstein frequency measured in specific heat. The value determined that way is  $0.44 \text{ W cm}^{-1} \text{ K}^{-1}$  (Open square in Fig. 2). The value quoted in the above table is  $\Lambda_{\min}$ , which is based on the measured speeds of sound (Open circle in Fig. 2). See text.

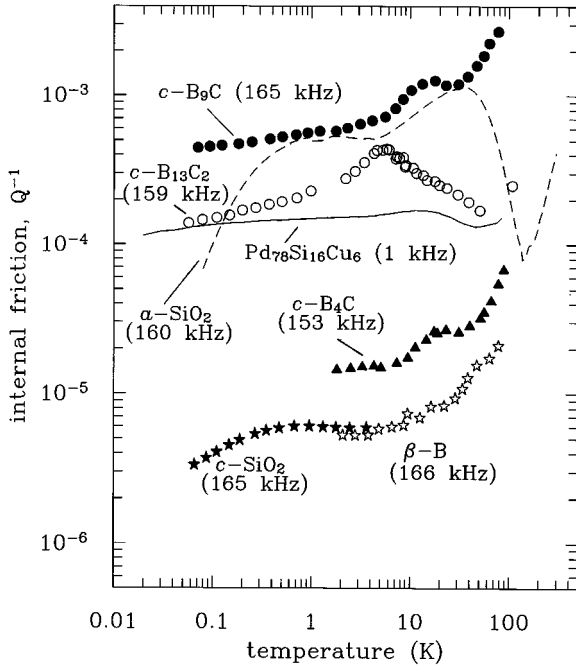


**FIG. 5.** Internal friction of crystalline  $c\text{-B}_{1-x}\text{C}_x$ , which shows a similar approach to glass-like behavior with increasing  $x$  as is seen in Fig. 3 for  $\text{Ba}_{1-x}\text{La}_x\text{F}_{2+x}$ . Data labeled  $c\text{-SiO}_2$  and  $\beta\text{-B}$  are clamping losses. The data for  $c\text{-B}_4\text{C}$  and the more carbon deficient carbides are the incremental internal frictions after the clamping losses have been subtracted as outlined in (6). The sources for the other data are given in the text.

the epoxy and in the metallic base of the oscillator. When a  $\beta\text{-B}$  polycrystal is attached to the quartz transducer, the internal friction in the temperature range of overlap does not change significantly, which indicates that the loss associated with  $\beta\text{-B}$  is much less than the clamping losses. With the  $c\text{-B}_4\text{C}$  sample on the torsional oscillator, the internal friction increases noticeably; in Fig. 5 the internal friction of the  $\text{B}_4\text{C}$  sample alone is plotted after subtracting the clamping losses (details can be found in (6)). The internal friction increases by over a factor of 10 for  $c\text{-B}_{13}\text{C}_2$  over that of  $\text{B}_4\text{C}$  approaching that of amorphous solids, although its temperature dependence differs somewhat from that of amorphous solids ( $\alpha\text{-PdSiCu}$  (28) and  $\alpha\text{-SiO}_2$  (5)). Finally, for  $c\text{-B}_9\text{C}$ , the internal friction shows not only the proper magnitude, but also the expected independence of temperature known for amorphous solids. A difference seems to exist when compared to  $\alpha\text{-SiO}_2$ , for which the internal friction decreases at the lowest temperatures. According to the theory (8), such a drop-off is expected when the shortest relaxation time for the tunneling defects becomes long relative to the period of oscillation. If the relaxation occurs only through the assistance of thermal phonons, the decrease should approach a  $T^3$  dependence at the lowest temperatures, in agreement with the data for  $\alpha\text{-SiO}_2$ . For the amorphous metal  $\text{PdSiCu}$ ,

however, conduction electrons can aid the relaxation process. For recent discussions of this point, see (29). The absence of a drop-off of the internal friction of  $c\text{-B}_9\text{C}$  suggests the presence of some additional medium aiding the relaxation, in addition to the thermal phonons. Conceivably, it could be the bi-polarons which have recently been found to be mobile even at helium temperatures (30).

The convincing evidence that the polycrystalline  $c\text{-B}_9\text{C}$  contains low energy tunneling states similar to those of amorphous solids is shown in Fig. 6. The bare double-paddle oscillator shows almost exclusively clamping losses below 10 K. The addition of a  $\sim 0.17\ \mu\text{m}$   $\alpha\text{-B}_9\text{C}$  film increases the damping of the oscillator by an order of magnitude. When the internal friction of the film itself is extracted from these data (6), it agrees in magnitude with that of  $c\text{-B}_9\text{C}$  and even shows a slight decrease with temperature at the lowest temperatures (compare with data for  $\alpha\text{-SiO}_2$  (31)).

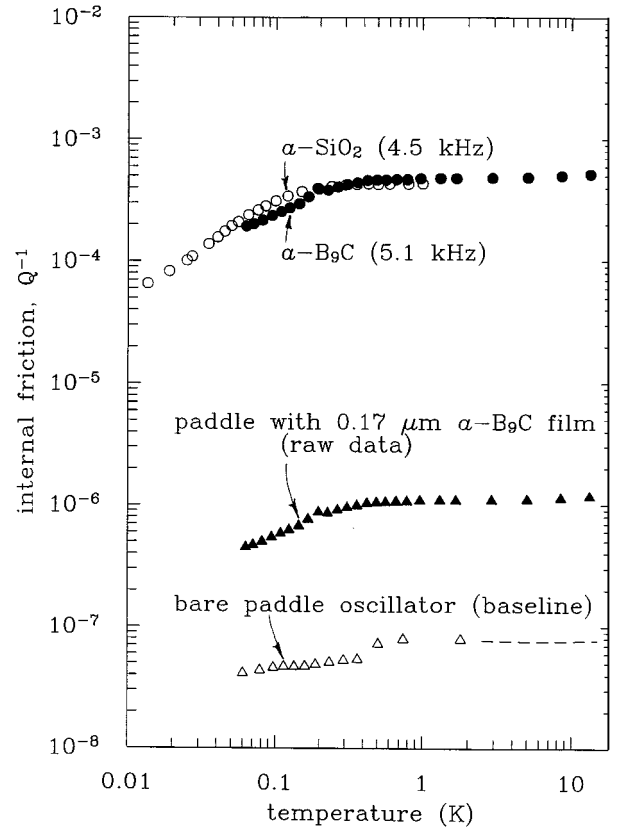


**FIG. 6.** Internal friction of a double-paddle oscillator before and after deposition of  $\sim 0.17\ \mu\text{m}$   $\alpha\text{-B}_9\text{C}$  film. The internal friction of the film itself is very similar to that of crystalline  $\text{B}_9\text{C}$  (Fig. 5), and closely resembles that of other amorphous solids, with  $\alpha\text{-SiO}_2$  shown for comparison. The latter was measured on a paddle etched out of a wafer of  $\alpha\text{-SiO}_2$  with a resonance frequency of the antisymmetric mode of 4.5 kHz (31).

## V. DISCUSSION

The measurements of the low temperature internal friction have shown that, with increasing carbon deficiency, low energy excitations occur in  $c\text{-B}_{1-x}\text{C}_x$ . This behavior resembles that found in other disordered crystals, as illustrated in Fig. 3 with  $\text{Ba}_{1-x}\text{La}_x\text{F}_{2+x}$ . The quantitative agreement of the tunneling states in the disordered crystalline  $c\text{-B}_9\text{C}$  with those observed in an amorphous film of  $\text{B}_9\text{C}$  provides quantitative proof that the  $c\text{-B}_9\text{C}$  has indeed low energy excitations equal to those of the amorphous phase.

From the resonance frequency of the compound torsional oscillator, we have determined a low temperature transverse sound speed  $v_t = 7.86 \times 10^5 \text{ cm s}^{-1}$  for  $c\text{-B}_9\text{C}$  (7% larger than the value by Gieske *et al.* quoted in (1)). From their values of transverse and longitudinal sound speeds and the number density of atoms, a minimum thermal conductivity  $\Lambda_{\min}$  at 300 K has been calculated (see Table 1) and is compared in Fig. 2 with the measured value (1). The good agreement of the measured value with the theoretical  $\Lambda_{\min}$ , in conjunction with the existence of the low energy tunneling excitations, is taken as convincing evidence for the existence of glass-like lattice vibrations in the crystalline  $c\text{-B}_9\text{C}$ . Random stresses of the kind conceivable in  $\text{Ba}_{1-x}\text{La}_x\text{F}_{2+x}$  can be postulated as possible origins of these excitations, but given the complex structure of  $c\text{-B}_9\text{C}$ , they are as difficult to quantify as in most disordered crystals with glass-like lattice vibrations, e.g., the feldspars. Nonetheless, given the fact that the existence of glass-like lattice vibrations in  $c\text{-B}_9\text{C}$  has now been shown conclusively, and given the experimental fact that the thermal conductivity of a crystal with glass-like lattice vibrations is close to that of  $\Lambda_{\min}$ , we may now conclude that no further decrease of the thermal conductivity through any further increase in the disorder in the boron carbides is to be expected.

## ACKNOWLEDGMENTS

We thank Dr. T. Aselage for providing the polycrystalline  $c\text{-B}_{1-x}\text{C}_x$  and Dr. B. E. White for the double-paddle oscillators used for studying the  $a\text{-B}_9\text{C}$  film. We also thank both of them for stimulating discussions. We thank Dr. K. A. Topp for calculations of the minimum thermal conductivity for several of the solids listed in Table 1, and also for many useful comments on the manuscript, and Dr. J. E. Van Cleve for permission to use his internal friction data on  $a\text{-SiO}_2$  shown in Fig. 6. This work was supported by the National Science Foundation (Grant DMR-91-1598), and through the Cornell Materials Science Center.

## REFERENCES

1. P. A. Medwick, H. E. Fischer, and R. O. Pohl, *J. Alloys Compounds* **203**, 67 (1994).
2. T. L. Aselage, D. R. Tallant, J. H. Gieske, S. B. Van Deusen, and R. G. Tissot, in "The Physics and Chemistry of Carbides, Nitrides, and Borides" (R. Freer, Ed.), p. 97. Kluwer, Dordrecht, 1990.
3. G. A. Samara, H. L. Tardy, E. L. Venturini, T. L. Aselage, and D. Emin, *Phys. Rev. B* **48**, 1468 (1993).
4. T. L. Aselage, private communication.
5. D. G. Cahill and J. E. Van Cleve, *Rev. Sci. Instrum.* **60**, 2706 (1989).
6. P. A. Medwick, B. E. White, Jr., and R. O. Pohl, submitted to *Phys. Rev. B*.
7. B. E. White, Jr. and R. O. Pohl, in "Thin Films: Stresses and Mechanical Properties V" (S. P. Baker *et al.*, Eds.), p. 567. Materials Research Society, Pittsburgh, PA, 1995.
8. S. Hunklinger and A. K. Raychaudhuri, in "Progress in Low Temperature Physics" (D. F. Brewer, Ed.), Vol. IX, p. 265. North Holland, Amsterdam, 1986.
9. W. A. Phillips, *Rep. Prog. Phys.* **50**, 1657 (1987).
10. J. F. Berret and M. Meissner, *Z. Phys. B—Condensed Matter* **70**, 65 (1988).
11. B. E. White and R. O. Pohl, *Phys. Rev. Lett.* **75**, 4437 (1995).
12. F. Birch and H. Clark, *Ann. J. Sci.* **238**, 528 (1940).
13. R. C. Zeller and R. O. Pohl, *Phys. Rev. B* **4**, 2029 (1971).
14. A. Einstein, *Ann. Phys.* **35**, 679 (1911).
15. P. W. Bridgman, "The Physics of High Pressure," p. 319. McMillan, New York, 1931.
16. D. G. Cahill and R. O. Pohl, *Solid State Comm.* **70**, 927 (1989).
17. D. G. Cahill, S. K. Watson, and R. O. Pohl, *Phys. Rev. B* **46**, 6131 (1992).
18. D. G. Cahill, R. B. Stephens, R. H. Tait, S. K. Watson, and R. O. Pohl, in "Thermal Conductivity 21," (C. J. Cramers and H. A. Fine, Eds.), p. 3. Plenum, New York, 1990.
19. A. K. Raychaudhuri and R. O. Pohl, *Phys. Rev. B* **46**, 10657 (1992).
20. P. A. Medwick, R. O. Pohl, and T. Tanaka, *Jpn. J. Appl. Phys. Ser. 10*, 106 (1994).
21. I. Higashi, K. Kobayashi, T. Tanaka, and Y. Ishizawa, *J. Solid State Chem.* **133**, 16 (1997).
22. D. G. Cahill and R. O. Pohl, *Phys. Rev. B* **39**, 10477 (1989).
23. K. A. Topp and D. G. Cahill, *Z. Phys. B* **101**, 235 (1997).
24. J. A. Harrington and C. T. Walker, *Phys. Rev. B* **1**, 882 (1970).
25. D. G. Cahill, J. R. Olson, H. E. Fischer, S. K. Watson, R. B. Stephens, R. H. Tait, T. Ashworth, and R. O. Pohl, *Phys. Rev. B* **44**, 12226 (1991).
26. J. R. Olson, K. A. Topp, and R. O. Pohl, *Science* **259**, 1145 (1993).
27. X. Lu, M. C. Arduni-Schuster, J. Kuhn, O. Nilsson, J. Fricke, and R. W. Pekala, *Science* **255**, 971 (1992).
28. A. K. Raychaudhuri and S. Hunklinger, *Z. Phys. B* **57**, 113 (1984).
29. S. N. Coppersmith and B. Golding, *Phys. Rev. B* **47**, 4922 (1993); G. Zarant, A. Zawadowski, *Phys. Rev. B* **50**, 932 (1994); D. C. Ralph and R. A. Buhrman, *Phys. Rev. B* **51**, 3554 (1995).
30. T. L. Aselage, S. S. McCreedy, and D. Emin, these proceedings; T. L. Aselage, private communication.
31. J. E. Van Cleve, Ph.D. thesis, Cornell University, 1991.